

Fig. 1 Postbuckling behavior and imperfection-sensitivity.

lem. In each case the abscissa is supposed to be a measure of the amplitude of a unique buckling mode corresponding to the buckling load associated with the lowest eigenvalue. The first two sketches illustrate symmetrical bifurcations, for which the initial postbuckling behavior is independent of the sign of the buckling displacement. Only symmetrical bifurcations occur in all of the problems of this paper, but asymmetrical bifurcations illustrated in the last sketch also are possible theoretically. The dotted curves show how the applied load varies with displacement when the structure contains an initial deflection in the shape of the buckling mode. If, as shown in the first sketch, the load on the perfect structure drops after buckling, then the load on the imperfect structure attains a local maximum that is lower than the classical buckling load of the perfect structure. Under dead loading, this local maximum would be associated with a sudden, possibly catastrophic, increase in displacement which, in a test, would be characterized as buckling. If, as in the case illustrated by the second sketch, the load on the perfect structure increases after buckling, the corresponding imperfect structure would exhibit a much milder growth of displacement as the load reaches and exceeds the classical buckling load. Finally, if the perfect structure has an asymmetric buckling bifurcation, snap buckling of the imperfect structure would be expected for one sign of the initial imperfection and mild behavior for the opposite sign. Because the buckling strengths of structures characterized by the behaviors shown in the first and the last of the sketches in Fig. 1 are influenced by initial imperfections, in some cases markedly so, such structures will be called imperfection-sensitive.

The extent to which imperfections can affect the buckling strengths of imperfection-sensitive shell structures is shown in Fig. 2. Suppose that the symmetrical postbuckling load displacement relation is given by the equation

$$P/P_c = 1 + b(\delta/t)^2 \quad (1)$$

where P_c is the classical buckling load; δ is the amplitude of the buckling displacement, say normal to the shell; and t is the shell thickness. The coefficient b is then a measure of the rapidity with which the load rises or drops after buckling. Imperfection-sensitive structures would, of course, be characterized by negative values of b . Let P_s be the buckling load of the imperfect structure when it contains an initial imperfection amplitude $\bar{\delta}$ in the shape of the buckling mode. Then the solid curves on the right of Fig. 2 show how the ratio P_s/P_c varies with the value of $\bar{\delta}/t$. As originally shown

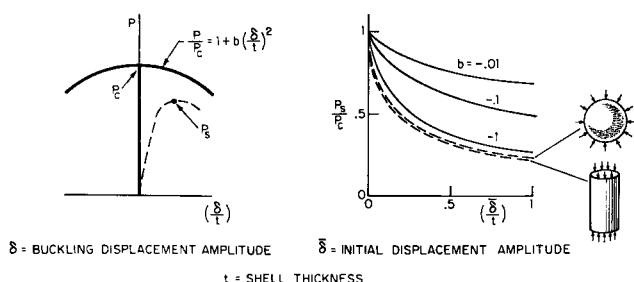


Fig. 2 Buckling of imperfection-sensitive shells.

by Koiter, these curves are governed by the equation

$$\left(1 - \frac{P_s}{P_c}\right)^{3/2} = \frac{3(3)^{1/2}}{2} (-b)^{1/2} \left|\frac{\bar{\delta}}{t}\right| \left(\frac{P_s}{P_c}\right) \quad (2)$$

and really should be regarded as correct only in an asymptotic sense for sufficiently small values of the initial displacement.

The most notorious imperfection-sensitive shell structure is probably the long thin-walled cylinder under axial compression which, as is well known, may buckle at values of stress that are small fractions of the classical buckling stress. Unfortunately, this system is not described by the simple sketches on the left of Fig. 2 because it has a multiplicity of buckling mode shapes associated with the classical buckling mode. However, a separate analysis, due to Koiter, gives the lower dotted curve on the right of Fig. 2 for the effect of initial axisymmetric imperfections on the buckling strengths of such cylinders. This curve provides a calibration for the significance of the coefficient b in the case of structures that have just one buckling mode associated with a symmetrical bifurcation. Thus, a value of $b = -1$ presumably would imply imperfection-sensitivity about as severe as that of a cylinder under axial compression. Note, however, that values of b between -0.1 and -1 evidently also would have quite significant implications, and even values of b in the neighborhood of -0.01 could imply buckling loads smaller than the classical ones by amounts that are not entirely negligible.

In passing, mention can be made of a recent study carried out on another structure that has multiple buckling modes associated with its classical buckling load, namely, the spherical shell under uniform external pressure. It has long been suspected that this structure is about as imperfection-sensitive as the cylindrical shell, and this has been verified theoretically very recently³ on the basis of, again, an asymptotic calculation based on Koiter's general theory; this theory exploits the shallow shell equations appropriate to very thin shells that buckle with very short wave lengths. The variation of P_s/P_c with $(\bar{\delta}/t)$ found for the imperfect sphere having a certain checkerboard pattern of initial displacements is given by the dotted curve just above, and nearly coincident with, the curve for the cylinder.

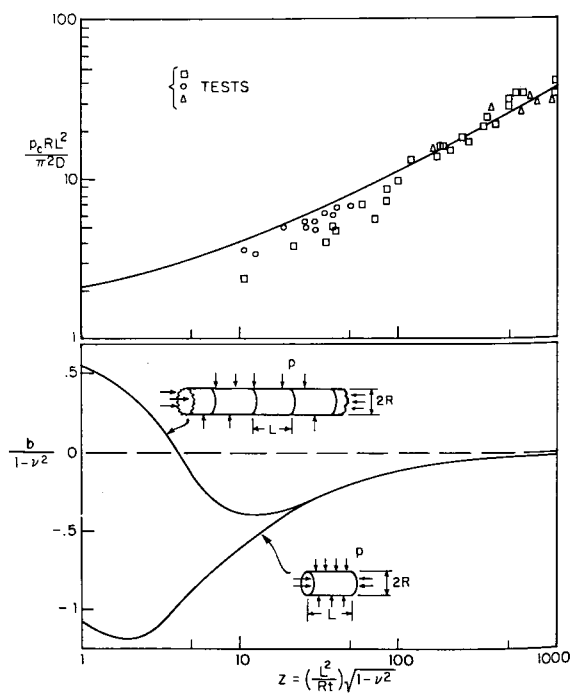


Fig. 3 Classical buckling and imperfection-sensitivity of simply supported cylinders under hydrostatic loading.

Attention now will be directed to the results of studies of several configurations having symmetrical buckling bifurcations with just one buckling mode. The point of these studies was to discover whether, and to what extent, these configurations are imperfection-sensitive by calculating the postbuckling coefficient b . All of these calculations were guided by the general theory of postbuckling behavior which was laid down by Koiter. Within the framework of the shell theories used (Donnell, shallow-shell, or a hybrid combination of these), the calculations were exact.

Simply Supported Cylinders under Hydrostatic Loading

The upper curve in Fig. 3 provides the classical hydrostatic buckling pressure P_c of a cylindrical shell having conventional simple support boundary conditions. The theoretical results for the nondimensional buckling pressure $P_c R L^2 / \pi^2 D$, calculated by Batdorf⁴ on the basis of Donnell's equations, are plotted against the curvature parameter Z , introduced by Batdorf. The results are equally applicable to an isolated shell of length L or to a very long shell continuous over rigid frames having a spacing of L which provides no torsional restraint to the cylinder. In each case, however, prebuckling deformations are neglected. The lower part of the figure displays the new results just found⁵ for the postbuckling coefficient b again plotted against Z . As shown, the parameter b is different for the two configurations even though the classical buckling pressure is the same; the isolated cylinder turns out to be substantially more imperfection-sensitive over the low range of Z than the cylinder continuous over frames. It might be mentioned that there have been previous investigations of the postbuckling behavior of cylinders under hydrostatic loading, with results that could be described as approximate solutions for finite postbuckling deformations. The present results, in contrast, are asymptotically exact solutions for vanishingly small postbuckling deflections. It is felt that this present kind of solution has greater significance and is perhaps more reliable as an index of imperfection-sensitivity.

The results of buckling tests from a variety of sources (as collected by Dow⁶) are displayed in Fig. 3 for comparison with the theoretical classical buckling pressures. The extent to which theory and experiment disagree in various ranges of Z is in qualitative agreement with the degrees of

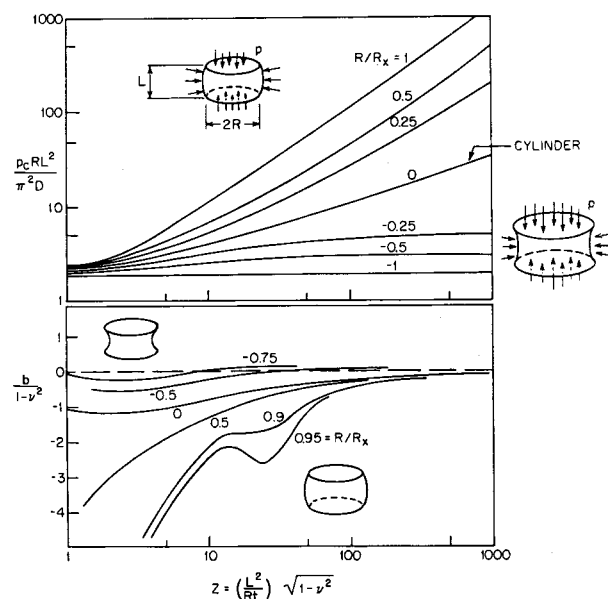


Fig. 4 Classical buckling and imperfection-sensitivity of simply supported toroidal segments under hydrostatic loading.

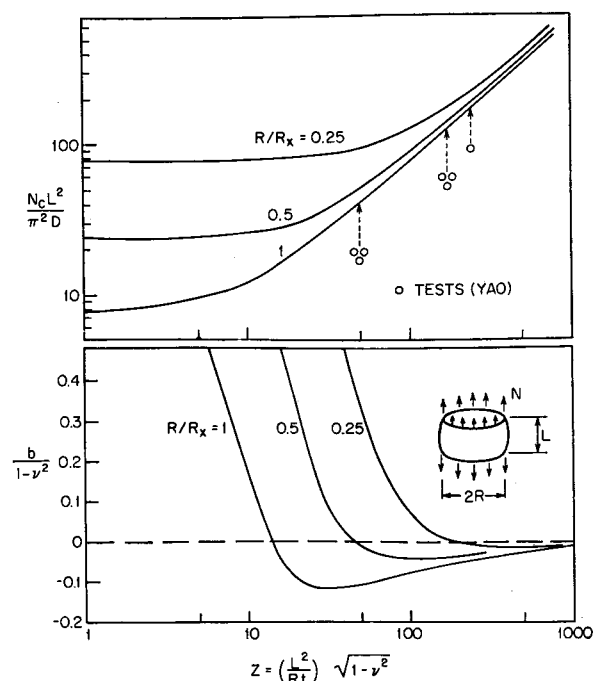


Fig. 5 Classical buckling and imperfection-sensitivity of simply supported toroidal segments under tension.

imperfection-sensitivity implied by the negative values of b in these ranges.

Toroidal Segments under Hydrostatic Loading

The top part of Fig. 4 shows results recently calculated by Stein and McElman⁷ for the classical hydrostatic buckling pressures of simply-supported toroidal segments having various curvature ratios R/R_x , where R represents the radius of the boundary circles, and $1/R_x$ is the meridional curvature. The case $R/R_x = 0$ coincides with the cylinder just discussed. The results of recent calculations⁸ of the postbuckling coefficient b are displayed in the bottom part of the figure. The most important implication here is that although the classical buckling pressure increases with increasing values of R/R_x , so does imperfection-sensitivity. In other words, increasing the meridional curvature of a toroidal shell would not strengthen the shell against buckling as much as one might hope for, on the basis of a classical buckling analysis alone. Note that as R/R_x approaches 1 from below, the spherical geometry is attained, for which postbuckling calculations, on the basis of a unique classical buckling mode, may no longer be valid, and so the curiously shaped curves for $R/R_x = 0.9$ and 0.95 should be discounted. It confidently may be concluded, however, that, for hydrostatic loading, imperfection-sensitivity disappears only for toroidal segments of sufficiently large negative Gaussian curvature.

Toroidal Segments under Axial Tension

For positive values of R/R_x , a toroidal segment under axial tension acquires circumferential compressive stresses and therefore is susceptible to buckling. The results of calculations⁸ for the classical axial buckling force per unit length N_c are shown as a function of Z in Fig. 5 for several values of R/R_x . The postbuckling coefficient b was found to vary, as shown in the bottom part of Fig. 5; for each value of R/R_x there is imperfection-sensitivity only for Z larger than the critical value for which b goes negative. Several tests have been performed by Yao⁹ for the case $R/R_x = 1$, with results shown by the circles. Yao's specimens were clamped, rather than simply supported, but his own calculated buckling loads for this case were only a little higher

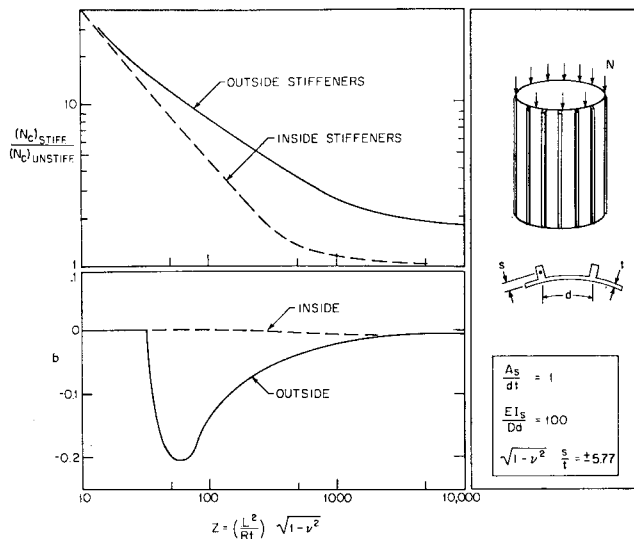


Fig. 6 Classical buckling and imperfection-sensitivity of simply supported stiffened cylinders under axial compression.

than those given by the curve in Fig. 5. Thus, the discrepancies between the test results and theoretically calculated buckling loads are consistent with the imperfection-sensitivity implied by the negative values of b ; these negative values were found for simply supported toroidal segments in the ranges of Z corresponding to the test specimens.

Stiffened Cylinders under Axial Compression

There has been much interest recently in the exciting re-discovery of van der Neut's early theoretical observation,¹⁰ now well confirmed by tests, that outside stringers can be much more effective than inside stringers in stiffening a circular cylinder against buckling under axial compression. It has been suggested occasionally that classical theories of buckling should be reliable for the quantitative prediction of the buckling loads of stiffened cylinders, regardless of whether the stiffeners are inside or outside. Recent calculations,¹¹ however, have shown this not to be so and an example is given in Fig. 6 for a simply supported cylinder. If torsional stiffness of the stringers is neglected, three parameters are needed to characterize the stiffening. These are the area ratio A_s/dt ; the bending stiffness ratio EI_s/Dt ; and the eccentricity ratio $(1 - \nu^2)^{1/2}(s/t)$ where s , the distance from the skin center line to the centroid of the stringer, is considered to be positive for outside stiffening and negative for inside stiffening. The values chosen for these nondimensional parameters in the present example correspond to only moderately heavy stiffening and are shown in Fig. 6. The curves at the top of Fig. 6 give, as a function of Z , the buckling load

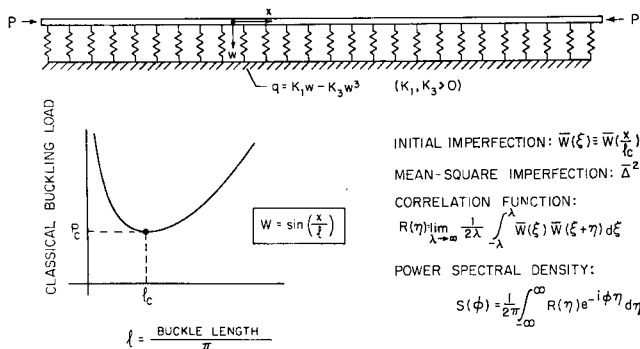


Fig. 7 Infinitely long column with random initial imperfections on a nonlinear foundation.

per unit circumference of the stiffened cylinder divided by the corresponding quantity for the unstiffened cylinder, and were calculated on the basis of "smeared-out" stiffener properties. These results imply the superiority of outside over inside stringers. This conclusion, however, clearly must be tempered by the results for the postbuckling coefficient b which show that the cylinder with outside stiffening generally is much more imperfection-sensitive than the one with inside stiffening. It should be emphasized that the coefficient b in this figure still is defined with respect to buckling displacements normalized by the skin thickness and not by any larger effective thickness of the shell-stringer combination. Consequently, over a substantial range of Z in the vicinity of 100, it appears that the effects of initial imperfections in reducing the strength of cylinders with outside stringers below the theoretically predicted classical buckling loads would be by no means negligible. On the other hand, it is interesting to note that in the range of high Z above 1000 both inside and outside stiffeners induce quite comparable imperfection-sensitivity, and so the benefits of outside stiffening would appear to be quite dependable in this range. In any event, the most important conclusion to be drawn is that, without supporting evidence, either experimental or theoretical, it would be quite incorrect to assume that classical buckling theory is adequate for the prediction of the buckling strength of stiffened cylinders under axial compression, especially if the stiffening is on the outside.

Structures with Random Imperfections

The kinds of investigations just discussed serve to demonstrate whether or not a given configuration is imperfection-sensitive but indicate only qualitatively the degree of such sensitivity; they can not be used to predict the actual buckling load of a given structure that is imperfection-sensitive. One reason for this deficiency is that the initial imperfection certainly does not have precisely the shape of the classical buckling mode, as assumed in the analyses. On the other hand, it does not seem very sensible to attempt to develop methods of analyses based upon a very detailed knowledge of the imperfection in the structure under consideration. A more useful goal might be to attempt to correlate the buckling strengths of imperfect structures with appropriate statistical descriptions of their initial imperfections. To that end the

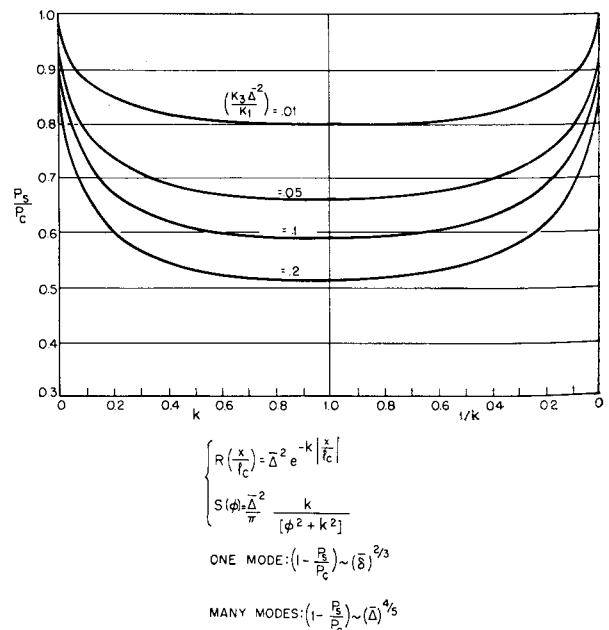


Fig. 8 Buckling loads of column with random imperfections.

pilot problem illustrated in Fig. 7 has recently been studied.¹² In this problem an infinitely long column rests on a nonlinear "softening" foundation and is supposed to have an initial displacement \bar{W} which is assumed to be a stationary random function of position along the length of the beam. The perfect structure has a continuous spectrum of buckling loads corresponding to the spectrum of buckle modes $\sin x/l$ where l can have any value. The critical buckling load P_C , however, occurs for a particular value l_c of this wavelength parameter. It is evident that not only will initial imperfections in the shape of the critical buckling mode influence the actual static buckling load of the imperfect structure, but so will, to some extent, imperfections having any other shape. It is supposed that the mean-square imperfection $\bar{\Delta}^2$ is known, as is the correlation function R of the imperfection (considered a function of the nondimensional parameter $\xi = x/l_c$). The associated power spectral density $S(\phi)$ is defined conventionally as the Fourier transform of the correlation function. The kinds of results that were found for this problem (by means of approximate techniques that lean heavily on the so-called "method of equivalent linearization") are illustrated in Fig. 8. Shown in this figure is one choice that was made (arbitrarily) for the correlation function of the imperfection, and the associated power spectral density, both characterized by the single parameter k in addition to the mean-square imperfection $\bar{\Delta}^2$. The mean-square imperfection combines with the parameters of the foundation modulus to give the pertinent nondimensional parameter $k_3\bar{\Delta}^2/k_1$ as a measure of the magnitude of the imperfection, and k serves as a measure of the spectral content of the imperfection. The curves show the calculated values of the ratio of the buckling load of the imperfect structure to that of the perfect structure as a function of these two parameters. It is interesting to note that the buckling loads are relatively insensitive to k over a substantial range. This tends to encourage the hope that quantitative predictions of the buckling strengths of imperfection-sensitive structures eventually may be possible on the basis of the knowledge of a few statistical parameters descriptive of the imperfections.

Noted in Fig. 8 is an interesting mathematical difference between these results for a structure having a continuous spectrum of buckling modes and the earlier ones for structures having unique buckling modes. In the one-mode case, the difference between the buckling loads of the perfect and imperfect structures is, asymptotically, proportional to $(\bar{\Delta})^{2/3}$; in the continuous-spectrum case this difference is proportional to $(\bar{\Delta})^{4/5}$.

Dynamic Buckling of Imperfection-Sensitive Structures

The general approach of Koiter recently has been extended by the writers¹³⁻¹⁵ to handle the buckling of imperfection-sensitive structures under a variety of time-dependent loading conditions. General results intended to serve as approximate guidelines for the analysis and design of such structures have thereby been obtained and just one example of this kind of result is illustrated in Fig. 9. Consider step-loading of an imperfection-sensitive structure of the type that, when perfect, bifurcates symmetrically as illustrated and, consequently, has a static buckling load P_S less than P_C if it is imperfect. The results of the dynamic analysis show that the same structure, having the same imperfection, would have a dynamic buckling load P_D given by the graph in Fig. 9. Here the ratio of the dynamic to the actual static buckling load of the imperfect structure is plotted against the ratio P_S/P_C , which, of course, equals 1 for the perfect structure and is smaller the more imperfect is the structure. It is seen that for step-loading the dynamic buckling load is always less than the static buckling load, but even for very imperfect structures it is never less than 70% of the static

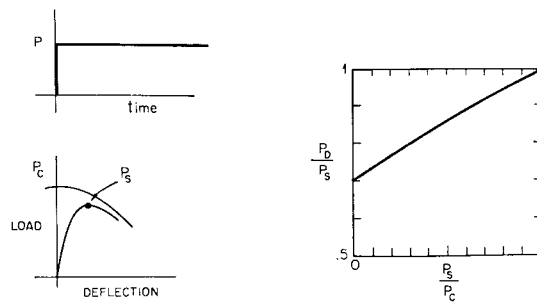


Fig. 9 Dynamic buckling, step loading.

buckling load. The most important and useful implication of this curve is that it provides an estimate of the dynamic buckling load just on the basis of P_S/P_C , and does not require a knowledge of the initial imperfection.

Spherical Cap under Concentrated Load

The last buckling problem to be discussed in this survey differs in several respects from all of those previously mentioned. The prebuckling stress state is not trivial, but requires the solution of a nonlinear problem; the buckling loads, themselves, have not been determined previously; and in all likelihood the structure is imperfection-insensitive, although this remains to be established theoretically. The clamped shallow spherical shell shown in Fig. 10 is subjected to a load P at the center; the solid curve shows how the value of the load parameter $P_C R/2\pi D$ associated with buckling varies with the conventional geometrical parameter λ . This curve gives the lowest of the loads given by the separate curves associated with buckling in various numbers n of circumferential waves. The case $n = 0$ for axisymmetric buckling has been obtained previously by Mescall,¹⁶ and corresponds to a local maximum in the variation of load with axisymmetric displacement. The other curves were found¹⁷ by discovering bifurcations of axisymmetric equilibrium paths into nonaxisymmetric branches. The mode shapes associated with the cases $n = 3, 4$, and 5 , when combined with an axisymmetric dimple, would correspond to deformed areas that are roughly in the shapes of triangles, squares, and pentagons, respectively. Such deformation shapes have, in fact, been observed in the past during tests on spherical shells under concentrated loads.^{18,19} There does not appear to be precise experimental information, however, concerning a critical value of load at which nonaxisymmetric deformations first begin to appear, nor has any snapping behavior been discovered in conjunction with their appearance. Indeed, observation has been made¹⁸ of a steady progression of three, four, and five lobed deflection patterns under increasing load, and this correlates with the competition shown in

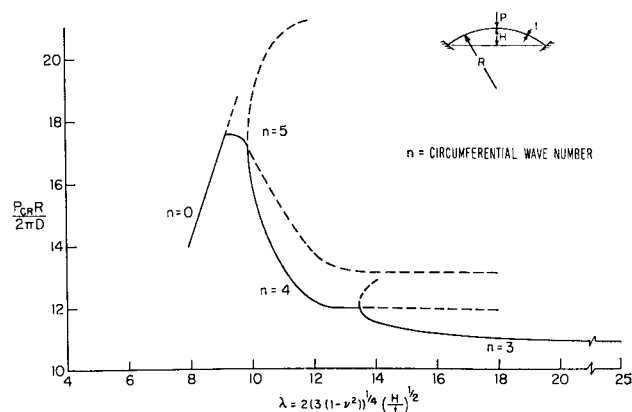


Fig. 10 Buckling loads for clamped spherical cap under concentrated load.

Fig. 10 among the modes for $n = 3, 4$, and 5. All of these facts suggest that the bifurcation into nonaxisymmetric deformation is associated with increasing values of load; and, verification of this imperfection-insensitive behavior on theoretical grounds now is in progress. It may be noted that the results for λ large are applicable to a full spherical shell of very small thickness. Thus, the full sphere under equal and opposite concentrated loads may be expected to begin to exhibit a transition from axisymmetric to nonaxisymmetric deformation at a value of $PR/2\pi D$ near 11.

References

- ¹ Koiter, W. T., "On the stability of elastic equilibrium," (in Dutch), Thesis, Delft, Amsterdam (1945).
- ² Koiter, W. T., "Elastic stability and post-buckling behavior," *Non-Linear Problems*, edited by R. E. Langer (University of Wisconsin Press, Madison, Wisc., 1963).
- ³ Hutchinson, J. W., "Imperfection-sensitivity of externally pressurized spherical shells," Harvard Univ., Rept. SM-5 (October 1965); also *J. Appl. Mech.* (to be published).
- ⁴ Batdorf, S. B., "A simplified method of elastic-stability analysis for thin cylindrical shells," NACA Langley Research Center Rept. 874 (1947); formerly NACA Langley Research Center TN 1341.
- ⁵ Budiansky, B. and Amazigo, J. C., "Initial post-buckling behavior of cylindrical shells under external pressure" (to be published).
- ⁶ Dow, D. A., "Buckling and post-buckling tests of ring-stiffened cylinders loaded by uniform external pressure," NASA Langley Research Center TN D-3111 (November 1965).
- ⁷ Stein, M. and McElman, J. A., "Buckling of segments of toroidal shells," *AIAA J.* **3**, 1704-10 (1965).
- ⁸ Hutchinson, J. W., "Initial post-buckling behavior of toroidal shell segments," Harvard Univ., Rept. SM-6 (November 1965); also *Intern. J. Solids Struct.* (to be published).
- ⁹ Yao, J. C., "Buckling of a truncated hemisphere under axial tension," *AIAA J.* **1**, 2316-20 (1963).
- ¹⁰ van der Neut, A., "General instability of stiffened cylindrical shells under axial compression," *Natl. Luchtraartlab.* **13**, Rept. S 314 (1947).
- ¹¹ Hutchinson, J. W. and Amazigo, J. C., "Imperfection-sensitivity of eccentrically stiffened cylindrical shells," Harvard Univ., Rept. SM-10 (April 1966).
- ¹² Fraser, W. B., "Buckling of a structure with random imperfections," Ph.D. Thesis, Harvard Univ. (1965).
- ¹³ Budiansky, B. and Hutchinson, J. W., "Dynamic buckling of imperfection-sensitive structures," *Proceedings of the XI International Congress on Applied Mechanics* (Julius Springer-Verlag, Berlin, to be published).
- ¹⁴ Hutchinson, J. W. and Budiansky, B., "Dynamic buckling estimates," *AIAA J.* **4**, 525-530 (1966).
- ¹⁵ Budiansky, B., "Dynamic buckling of elastic structures: criteria and estimates," Harvard Univ., Rept. SM-7 (January 1966); also *Proceedings of the International Conference on Dynamic Stability Structures* (Pergamon Press, New York, to be published).
- ¹⁶ Mescall, J. F., "Large deflections of spherical shells under concentrated loads," *J. Appl. Mech.* **32**, 936-938 (December 1965).
- ¹⁷ Fitch, J. R., "Buckling and post-buckling behavior of spherical caps under concentrated loads," Ph.D. Thesis, Harvard Univ. (research in progress).
- ¹⁸ Penning, F. A. and Thurston, C. A., "The stability of shallow spherical shells under concentrated loads," Martin-Marietta Corp., NASA Contractor Rept. CR-265 (July 1965).
- ¹⁹ Evan-Ivanovski, R. M., Cheng, H. S., and Loo, T. C., "Experimental investigations on deformations and stability of spherical shells subjected to concentrated loads at the apex," *Proc. 4th U. S. Natl. Cong. Appl. Mech.* **1**, 563-575 (1962).